AMERICAN SOCIETY FOR MICROBIOLOGY | Applied and Environmental Microbiology®

GEOMICROBIOLOGY

Microbially Mediated Coupling of Fe and N Cycles by Nitrate-Reducing Fe(II)-Oxidizing Bacteria in Littoral Freshwater Sediments

Franziska Schaedler,[a] Cindy Lockwood,[a] Ulf Lueder,[a] Clemens Glombitza,[b,c] Andreas Kappler,[a,b] Caroline Schmidt[a]

[a]Geomicrobiology, Center for Applied Geosciences, University of Tübingen, Germany
[b]Center for Geomicrobiology, Department of Bioscience, Aarhus University, Aarhus, Denmark
[c]NASA Ames Research Center, Moffett Field, California, USA

ABSTRACT Nitrate-reducing iron(II)-oxidizing bacteria have been known for approximately 20 years. There has been much debate as to what extent the reduction of nitrate and the oxidation of ferrous iron are coupled via enzymatic pathways or via abiotic processes induced by nitrite formed by heterotrophic denitrification. The aim of the present study was to assess the coupling of nitrate reduction and iron(II) oxidation by monitoring changes in substrate concentrations, as well as in the activity of nitrate-reducing bacteria in natural littoral freshwater sediment, in response to stimulation with nitrate and iron(II). In substrate-amended microcosms, we found that the biotic oxidation of ferrous iron depended on the simultaneous microbial reduction of nitrate. Additionally, the abiotic oxidation of ferrous iron by nitrite in sterilized sediment was not fast enough to explain the iron oxidation rates observed in microbially active sediment. Furthermore, the expression levels of genes coding for enzymes crucial for nitrate reduction were in some setups stimulated by the presence of ferrous iron. These results indicate that there is a direct influence of ferrous iron on bacterial denitrification and support the hypothesis that microbial nitrate reduction is stimulated by biotic iron(II) oxidation.

IMPORTANCE The coupling of nitrate reduction and Fe(II) oxidation affects the environment at a local scale, e.g., by changing nutrient or heavy metal mobility in soils due to the formation of Fe(III) minerals, as well as at a global scale, e.g., by the formation of the primary greenhouse gas nitrous oxide. Although the coupling of nitrate reduction and Fe(II) oxidation was reported 20 years ago and has been studied intensively since then, the underlying mechanisms still remain unknown. One of the main knowledge gaps is the extent of enzymatic Fe(II) oxidation coupled to nitrate reduction, which has frequently been questioned in the literature. In the present study, we provide evidence for microbially mediated nitrate-reducing Fe(II) oxidation in freshwater sediments. This evidence is based on the rates of nitrate reduction and Fe(II) oxidation determined in microcosm incubations and on the effect of iron on the expression of genes required for denitrification.

KEYWORDS denitrification, iron cycling, iron metabolism, iron(II) oxidation, nitrate-dependent iron oxidation

Iron is the most abundant redox-active element in the Earth's crust. It occurs naturally as ferrous iron (Fe[II]) and ferric iron (Fe[III]) (1, 2). Under circumneutral pH conditions, Fe is cycled between these two oxidation states by a variety of biotic and abiotic reactions (3, 4). Abiotic reactions include the oxidation of Fe(II) by O_2, reactive N species, or Mn(IV), as well as the reduction of Fe(III) by humic substances or by light-induced reactions (2, 3, 5). Microbial redox cycling of iron includes the oxidation of iron by

Received 12 September 2017 **Accepted** 31 October 2017

Accepted manuscript posted online 3 November 2017

Citation Schaedler F, Lockwood C, Lueder U, Glombitza C, Kappler A, Schmidt C. 2018. Microbially mediated coupling of Fe and N cycles by nitrate-reducing Fe(II)-oxidizing bacteria in littoral freshwater sediments. Appl Environ Microbiol 84:e02013-17. https://doi.org/10.1128/AEM.02013-17.

Editor Volker Müller, Goethe University Frankfurt am Main

Address correspondence to Caroline Schmidt, caroline.schmidt@uni-tuebingen.de.

microaerobic (6), phototrophic (7), or nitrate-reducing Fe(II)-oxidizing bacteria (8) and the reduction of iron by Fe(III)-reducing bacteria that can grow either heterotrophically with organic carbon or autotrophically using hydrogen as electron donor and CO_2 as carbon source (9, 10).

The Fe cycle is of great importance, as the speciation of Fe and the properties of Fe minerals that are formed or dissolved by biotic or abiotic reactions can affect the availability of nutrients and trace elements (11, 12). Furthermore, the Fe cycle is coupled to many other elementary cycles, such as the C and N cycles (5, 13). Recently, the role of microbes in the coupling of Fe and N cycling has been questioned (14–16). This is because many cultures of nitrate-reducing Fe-oxidizing bacteria can only grow mixotrophically with an organic cosubstrate (13, 17, 18). The oxidation of Fe was thus suggested to be an abiotic side-reaction (14). This hypothesis is strengthened by the fact that all heterotrophic nitrate-reducing bacterial cultures seem to be capable of oxidizing Fe(II) (19). Furthermore, unlike microaerophilic Fe(II) oxidizers and photoferrotrophs, most nitrate-reducing Fe(II)-oxidizing bacteria lack mechanisms to prevent cell encrustation in Fe(III) minerals (20, 21). This missing adaptation was interpreted as indication of unintentional Fe(II) oxidation caused by nitrite accumulation during nitrate reduction, yet new findings suggest that no significant encrustation of nitrate-reducing Fe(II)-oxidizing bacteria occurs during autotrophic growth (22).

So far, the only known laboratory culture that can be maintained over the long term under autotrophic conditions is the enrichment culture KS. Additionally, several pure cultures which are capable of autotrophic nitrate-reducing Fe(II) oxidation have been described (8, 23–29). However, the ability for continuous Fe(II) oxidation and autotrophic growth over several generations has not yet been shown for all these cultures. Very recently the existence of autotrophic nitrate-reducing Fe(II)-oxidizing bacteria has also been demonstrated for a coastal marine sediment (30). This suggests the existence of a mechanism for enzymatic Fe(II) oxidation coupled to nitrate reduction and raises the question of whether this process is unique to marine sediments or also occurs in other environmental habitats, such as freshwater sediments.

In the present study, we assessed the influence at the molecular level of iron(II) on the nitrate-reducing members of a bacterial community. This was achieved by following Fe and dissolved N species over time in microcosm incubations with littoral freshwater sediment from Lake Constance, Germany. Additionally, we used molecular approaches to quantify abundances and activity levels of nitrate-reducing community members.

RESULTS

Geochemical properties of sediment, pore water, and overlying water. Lake Constance littoral sediment consists mainly of quartz sand (see Fig. S1 in the supplemental material) with 54.8% ± 2.2% silica by weight (see Table S1 in the supplemental material). It has a sandy structure (Fig. 1), with a pore water content of 22.1% ± 4.3% in the top 3 cm (see Table S1 in the supplemental material). The total iron content of the dry sediment was 1.4% ± 0.2% (Table S1). The top 1.5 mm of the sediment was oxic, containing up to 267.5 ± 0.9 μmol per liter O_2 (Fig. 1A). Consequently, the dissolved Fe(II) in the pore water ranged from 184.3 ± 8.4 μM in the oxic top 1.5 mm to 230 ± 4.1 μM in the lower anoxic layers, where it remained constant (Fig. 1D). In the overlying water the dissolved organic carbon (DOC) content was 1.8 ± 0.0 mg per liter and the sedimentary total organic carbon (TOC) content was 1.6%. The dissolved nitrate concentration in the overlying water was 52.5 ± 1.1 μM, and neither nitrite nor dissolved Fe(II) were detected.

Nitrate and nitrite concentrations in microbially active microcosms over time. In order to determine the influence of Fe(II) and Fe(III) on microbial denitrification we followed nitrate and nitrite concentrations in microcosm setups amended with different combinations of nitrate or nitrite and Fe(II) or Fe(III). The high reactivity of nitrate and nitrite, together with the time-consuming setup of the microcosm experiments until the first samples could be analyzed, would lead to a discrepancy between the

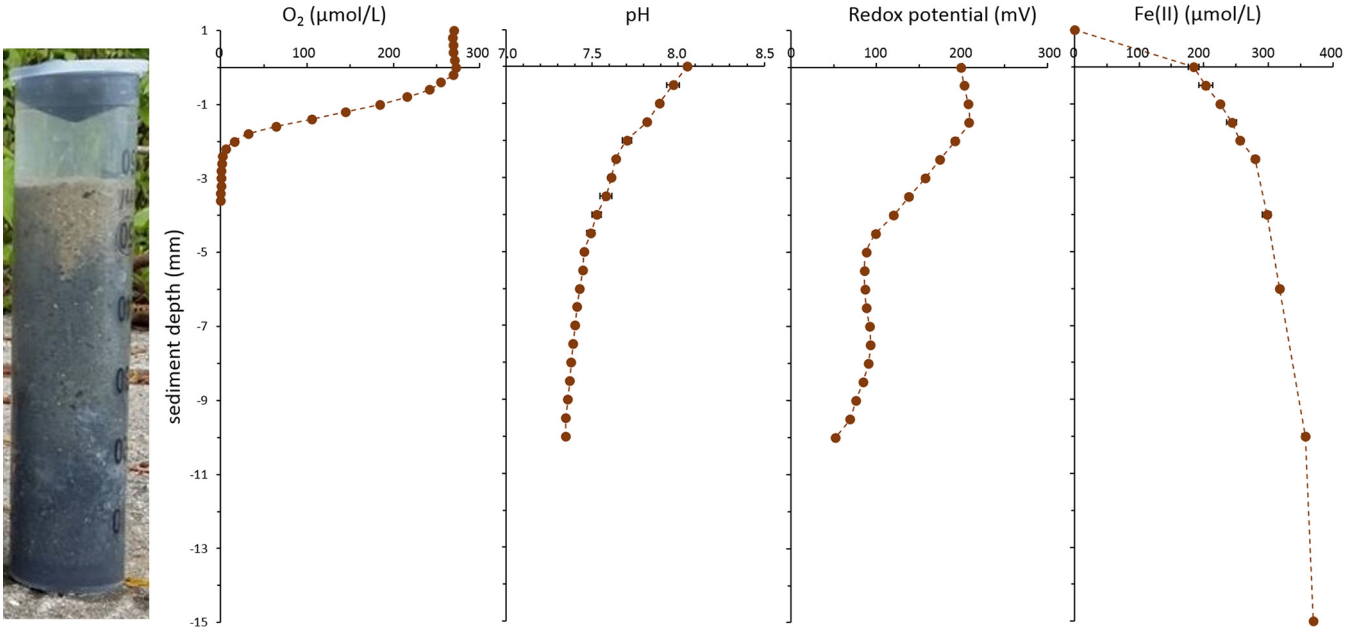

FIG 1 Oxygen, pH, redox potential (relative to the standard hydrogen electrode [SHE]), and Fe(II) profiles measured in Lake Constance littoral sediment cores (error bars indicate standard deviation of triplicate profiles).

concentrations added in amended microcosms and the measured time-zero (t_0) concentrations. No additional organic carbon was added.

All setups amended with nitrate showed complete removal of 2 mM nitrate and the simultaneous production of approximately 0.25 mM nitrite (Fig. 2B, C, and E). In microcosms amended with nitrate only, nitrate removal took 11 days at an average nitrate consumption rate of 245.7 ± 27.5 μM per day (Fig. 2B). With Fe(II) present in addition to nitrate (Fig. 2C), nitrate removal was completed after 7 days at an average

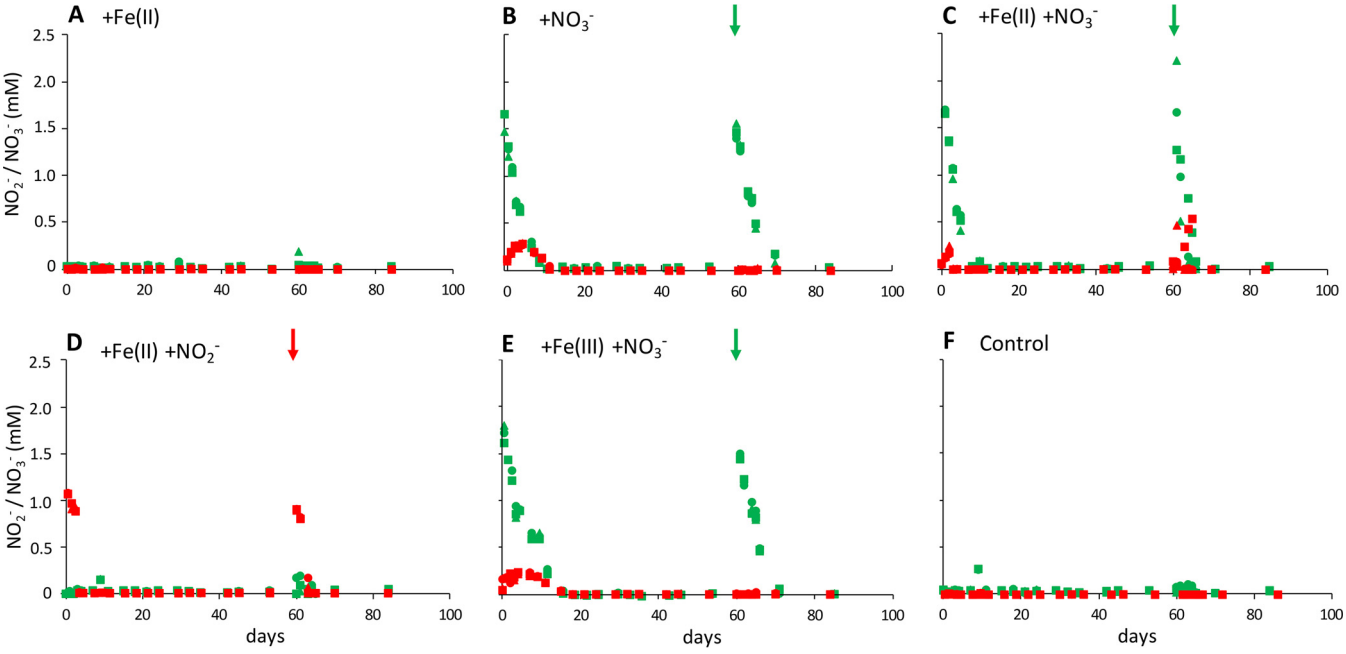

FIG 2 Nitrate (green) and nitrite (red) concentrations in different microcosm setups (triplicates shown with triangle, square, and diamond symbols). After the initial amendment (5 mM each Fe(II) and Fe(III) in addition to 1 mM derived from the sediment, 2 mM each nitrate and nitrite), microcosms were spiked with nitrate or nitrite at day 60 (see arrows). Fe conversion data of the same experiments are shown in Fig. 3.

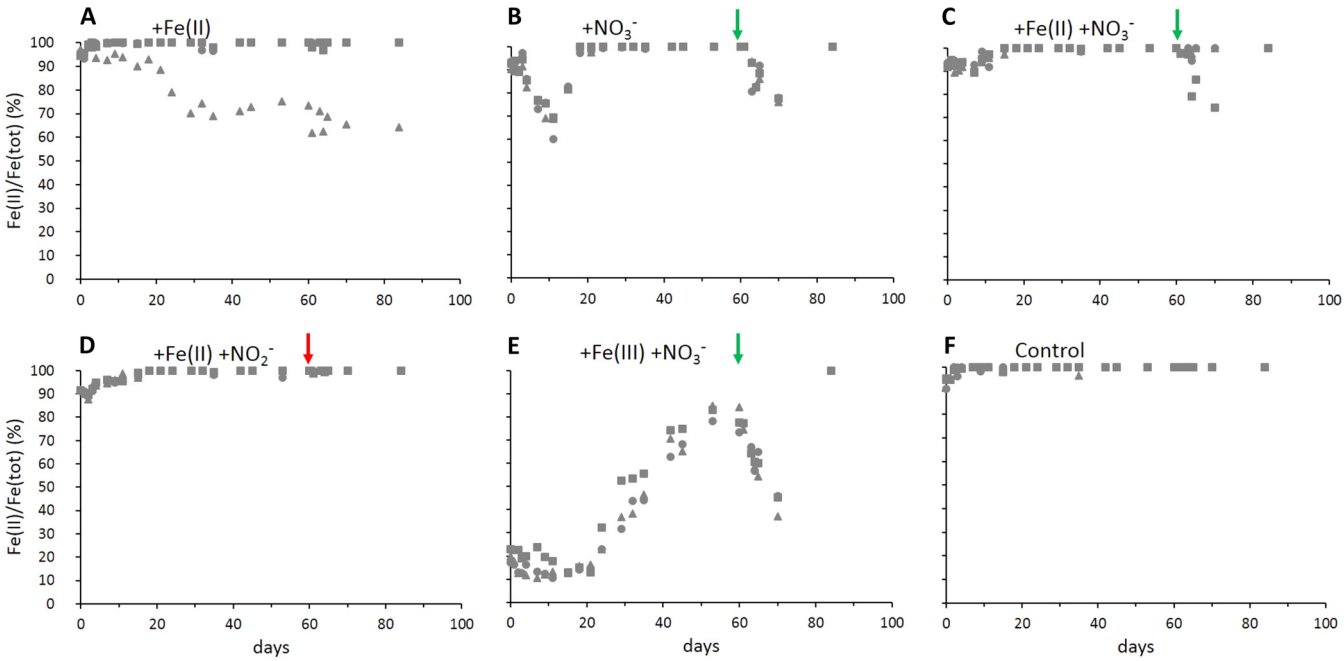

FIG 3 Fe(II)/Fe(tot) ratios in different microcosm setups (triplicates shown with triangle, square and diamond symbols). After the initial amendment (5 mM each Fe(II) and Fe(III) in addition to 1 mM derived from the sediment, 2 mM each nitrate and nitrite), microcosms were spiked with nitrate or nitrite at day 60 (see arrows). Nitrate and nitrite consumption of the same experiments are shown in Fig. 2. Fe(tot), total iron.

rate of 307.6 ± 12.9 μM per day while with Fe(III) present (Fig. 2E) nitrate removal took 15 days at an average rate of 218.4 ± 20.4 μM per day. After an additional spike with 2 mM nitrate at day 60, nitrate removal patterns were similar (Fig. 2), yet nitrite production was only observed in setups amended with both nitrate and Fe(II) (Fig. 2C). In microcosms amended with both nitrite and Fe(II), 2 mM nitrite was completely removed within 3 days at a nitrite consumption rate of 502.8 ± 12.6 μM per day (Fig. 2D). A similarly fast nitrite removal was observed after a second nitrite spike at day 60. In setups without nitrate or nitrite amendment (Fig. 2A and F), both nitrate and nitrite remained constant in the low μM range.

Fe speciation over time in microbially active setups. Microcosms spiked initially with only nitrate contained on average 1.17 ± 0.59 mM total natural Fe, of which 7.7% ± 1.4% was Fe(III) derived from the sediment (Fig. 3B). On average 34% ± 5% of the natural Fe was oxidized within 11 days, in parallel to nitrate consumption (Fig. 2B). After these first 11 days, Fe(III) was completely reduced to Fe(II) within the following 7 days. Following the nitrate spike at day 60, Fe(II) oxidation and rereduction of the formed Fe(III) showed a similar pattern, i.e., Fe(II) was oxidized over 10 days, concomitant with nitrate consumption, and the formed Fe(III) was completely rereduced afterwards. In microcosms amended with both nitrate and Fe(II), the starting Fe concentration was 4.63 ± 0.46 mM Fe, of which 7.5% ± 0.8% was Fe(III) (Fig. 3C). After 7 days, again concomitant with nitrate consumption (Fig. 2C), 9.4% ± 1.5% of the total Fe was oxidized, and subsequently all Fe(III) was completely rereduced within 8 days. After spiking again with nitrate at day 60, 2 replicates showed oxidation of only 2 to 5% Fe(II) over 4 days, followed by immediate Fe(III) reduction. In one replicate that showed slower nitrate removal, 25.8% Fe(II) was oxidized over 10 days and subsequently completely rereduced to Fe(II) (Fig. 3C). In microcosms amended with nitrate and the Fe(III) mineral ferrihydrite (Fig. 3E), oxidation of the complete sediment Fe(II) was observed during nitrate reduction. Rereduction of all Fe(III) present started at day 21, with a lag phase of 6 days after nitrate was completely reduced. Over 32 days, 82.0% ± 2.8% of the total Fe was reduced. After spiking with nitrate at day 60, Fe(II) oxidation started immediately, resulting in a maximum of 57.3% ± 4.0% Fe(III) within 10 days,

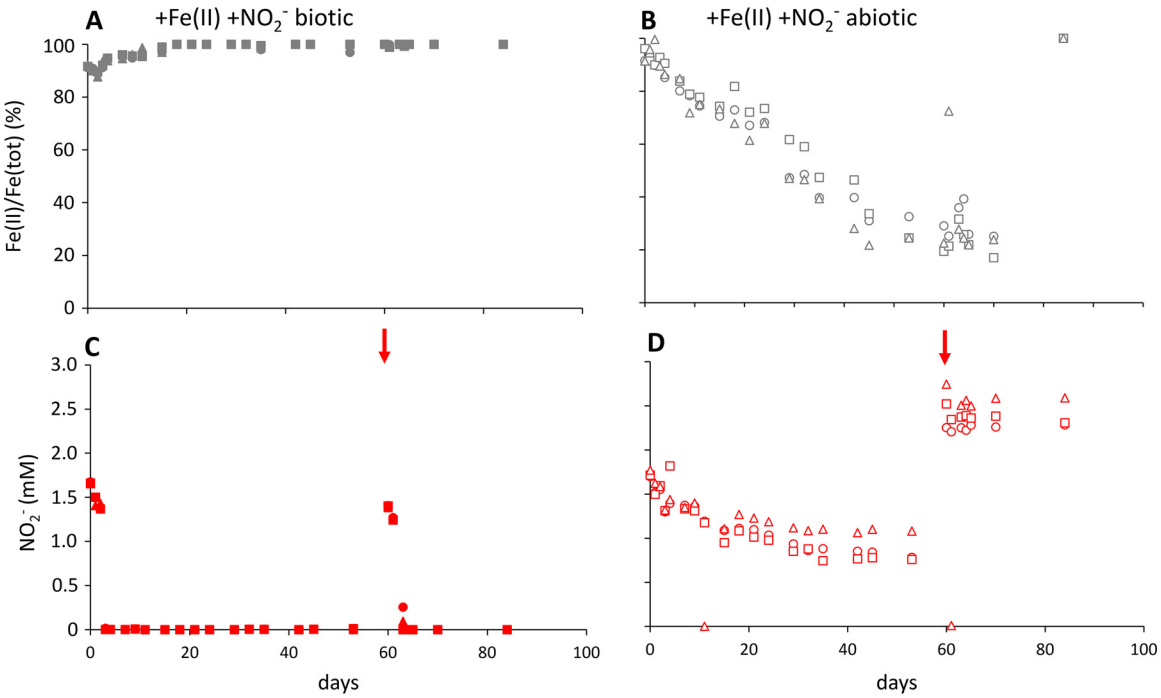

FIG 4 Nitrite concentrations (red) and Fe(II)/Fe(tot) ratios (gray) in biotic (filled symbols, left) and abiotic (open symbols, right) setups over time (triplicates shown with triangle, square, and diamond symbols). After the initial amendment (5 mM Fe[II], 2 mM nitrite), microcosms were spiked with nitrite at day 60 (see arrows).

which was subsequently rereduced. In microcosms amended with Fe(II) and nitrite (Fig. 3D), 11.2% ± 0.8% Fe was oxidized within 2 days and immediately completely rereduced. After a second nitrite spike on day 60, no oxidation of Fe(II) was observed. In setups amended with only Fe(II) and no nitrate (Fig. 3A), Fe(II) remained constant in two replicates, and one replicate showed slow and steady oxidation of 36% of the Fe(II) over the entire incubation time of 82 days. In unamended controls (Fig. 3F), the initially present Fe was fully reduced to 100% Fe(II) and remained as Fe(II) over the whole incubation time.

Abiotic oxidation of Fe(II) by nitrite. To assess the extent to which the oxidation of Fe(II) that occurs during the reduction of nitrate might be caused by abiotic reactions with nitrite, both Fe and nitrite were monitored over time in microcosms sterilized by autoclaving. Over 53 days, 0.86 ± 0.18 mM nitrite (of the added 2 mM) was removed together with the oxidation of 72.8% ± 3.8% of the initially present 5.04 mM Fe(II) (Fig. 4B and D). This corresponds to a Fe(II) oxidation rate of 74.5 ± 10.1 μM per day. After spiking with 2 mM nitrite on day 60, both nitrite and Fe(II) remained constant.

Consumption and production of organic matter. Volatile fatty acids (VFA) and dissolved organic carbon (DOC) were quantified over time to link Fe(II) oxidation and Fe(III) reduction to the bioavailability of organic carbon. Organic carbon was not amended, and all concentrations measured are derived from the sediment.

Initial DOC concentration in the overlying water was 10.7 ± 0.6 mg per liter. The highest DOC levels of 21.9 ± 2.5 mg per liter were measured after 45 days in microcosms amended with nitrite and Fe(II), while the lowest levels of 2.4 ± 0.3 mg per liter were found after 12 days in microcosms amended with nitrate and Fe(III). In setups amended with only Fe(II) as well as in unamended controls (Fig. 5A and F), DOC concentrations decreased constantly over 45 days of incubation. In all setups amended with nitrate (Fig. 5B, C, and E), DOC decreased during nitrate reduction over the first 12 days. After nitrate reduction ceased, DOC strongly increased in setups amended with nitrate and Fe(II) (Fig. 5C). In setups with only nitrate or nitrate and Fe(III) (Fig. 5B and

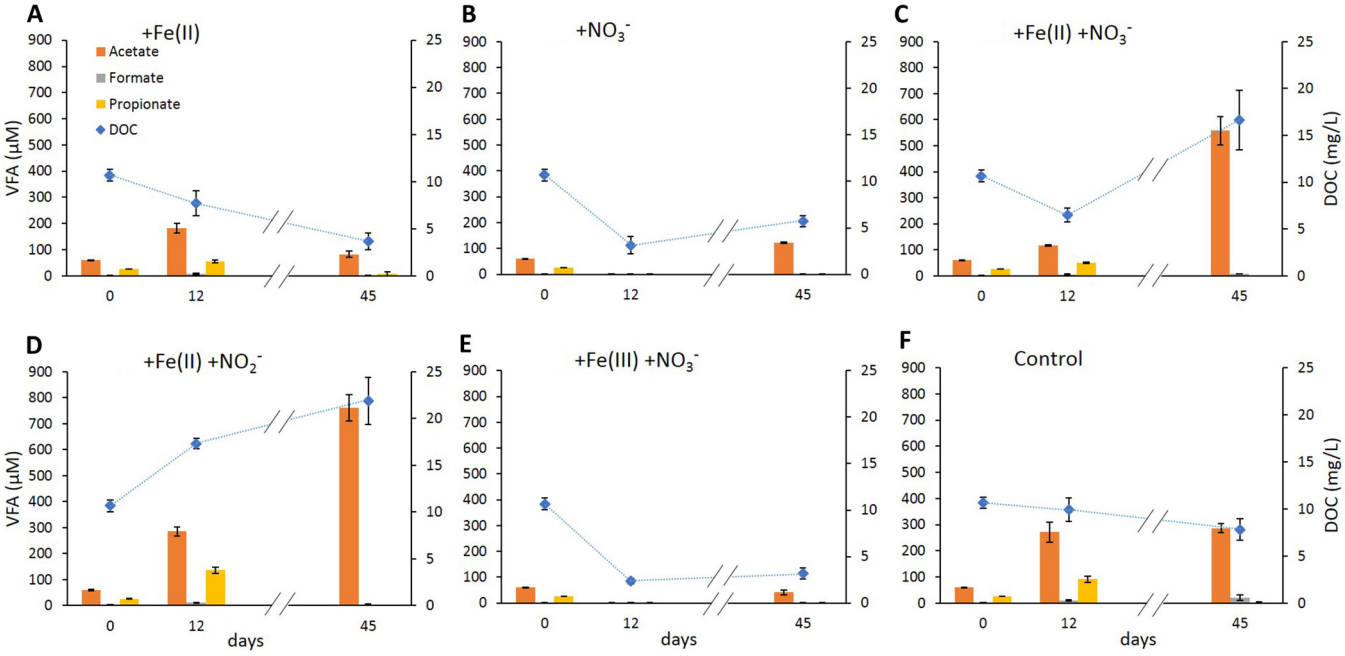

FIG 5 Concentrations of dissolved organic carbon (blue diamond symbols) and volatile fatty acids (bars) over time in different microcosm setups.

E), DOC increased only slightly after nitrate reduction was completed. Only in the setups that were amended with Fe(II) and nitrite (Fig. 5D) did the DOC increase constantly during 45 days of incubation.

The initial total concentration of all analyzed VFAs (acetate, formate, propionate, butyrate, isobutyrate, pyruvate, lactate, and valerate) in the microcosms was 89.5 ± 3.7 μM. As with the DOC values, the highest total VFA concentrations of up to 800.0 ± 45.9 μM were measured after 45 days of incubation in setups amended with Fe(II) and nitrite. The lowest concentrations (3.1 ± 0.9 μM) were measured in microcosms amended with nitrate after 12 days of incubation. All samples were dominated by acetate (76.7% ± 21.5% of the total VFA), which also resembled the overall trends.

Abundance and activity of nitrate- and nitrite-reducing bacteria. In order to assess whether Fe impacts microbial denitrification at a molecular level over time, we quantified gene copy numbers and gene transcripts of 16S rRNA genes, as well as functional genes encoding periplasmic nitrate reductase (*napA*), membrane-bound nitrate reductase (*narG*), copper-dependent nitrite reductase (*nirK*), and cytochrome cd_1 nitrite reductase (*nirS*). We found that abundances of all monitored genes remained mostly constant over the measured time points in all setups. Slight changes in overall bacterial abundances (16S rRNA) were reflected in abundances of the functional genes (Fig. 6). Gene expression levels of all functional genes, i.e., the proportion of DNA gene copies represented as cDNA, were between 1.1% and 1.7% in the natural sediment. In control setups without substrate amendment (Fig. 6F), expression levels decreased within the first 12 days of incubation and subsequently stayed constant below 0.5%. Overall, gene expression levels increased over the first 12 days of incubation and then decreased to levels similar to those in the unamended controls. Fe(II) alone (Fig. 6A) triggered a greater increase in gene expression levels of all functional genes, greater than that triggered by nitrate alone (Fig. 6B) or by Fe(II) in combination with nitrate (Fig. 6C). The highest expression levels, 19.9% for *napA* and 11.7% for *nirS*, were measured in microcosms amended with Fe(II) and nitrite (Fig. 6D). Only the microcosms amended with Fe(III) and nitrate (Fig. 6E) showed expression levels at day 45 higher than the starting levels. Expression levels at day 12 could not be determined in these setups due to too-low RNA concentrations.

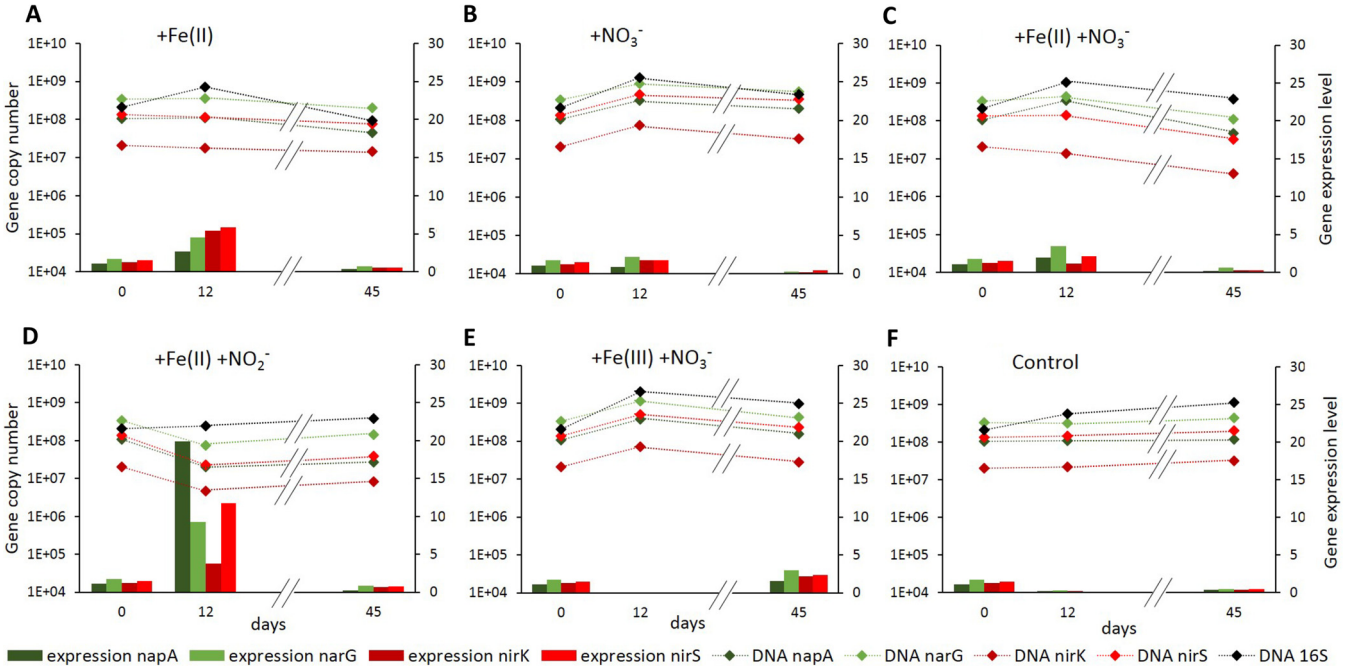

FIG 6 Gene abundances (diamond symbols) of genes encoding nitrate (*napA* and *narG*) and nitrite reductases (*nirK* and *nirS*) and bacterial 16S rRNA and expression levels, i.e., cDNA/DNA ratios (bars) of the nitrate- and nitrite-reductase-encoding genes over time in different microcosm setups over time. On day 12 the extracted RNA levels for setups amended with Fe(III) and nitrate were too low for further processing and quantification.

DISCUSSION

Dependence of microbial Fe(II) oxidation on the presence of nitrate and nitrite. Our experiments clearly showed that the oxidation of Fe(II) depends on the simultaneous reduction of nitrate or nitrite. No oxidation of Fe(II) could be observed in most setups without amendment of nitrate or nitrite (Fig. 2 and 3A and F) whereas in nitrate-spiked setups Fe(II) oxidation was limited to the duration of nitrate reduction. One replicate of the setup amended with only Fe(II) showed slow and steady Fe(II) oxidation (Fig. 3A), yet this replicate showed a distinct oxidation ring at the liquid surface, indicating an air leak and subsequent abiotic oxidation of Fe(II). As soon as nitrate or nitrite was completely used up, net Fe(II) oxidation ceased, and net Fe(III) reduction remained the dominating Fe-converting process in all setups. We also did not see a correlation between Fe(II) oxidation and the accumulation of nitrite, which has been previously reported as the main driver of abiotic Fe(II) oxidation during nitrate reduction (21).

The oxidation of iron coupled to the reduction of nitrate is based on the following stoichiometry: $10\ Fe^{2+} + 2\ NO_3^- + 24\ H_2O \rightarrow 10\ Fe(OH)_3 + N_2 + 18\ H^+$

According to this equation, a ratio of $NO_3^-{}_{(reduced)}/Fe(II)_{(oxidized)}$ of 0.2 is expected if nitrate reduction is coupled completely to Fe(II) oxidation (30), while for heterotrophic nitrate reduction the ratios are expected to be higher. As further described in Laufer et al. (31), this ideal ratio is expected to be even lower due to the fact that the electrons resulting from the oxidation of Fe(II) cannot be used exclusively for the reduction of nitrate but also feed into CO_2-fixing reactions that produce biomass, in particular in autotrophic nitrate-reducing Fe(II) oxidizers.

In microcosms amended with nitrate only or with both nitrate and Fe(II), the reduction of 2 mM nitrate was coupled to the oxidation of approximately 0.4 mM Fe (Fig. 2B and C and 3B and C), corresponding to an $NO_3^-{}_{(reduced)}/Fe(II)_{(oxidized)}$ ratio of 5. This implies that a significant part of the nitrate reduction was performed heterotrophically. After spiking again with 2 mM nitrate on day 60, the $NO_3^-{}_{(reduced)}/Fe(II)_{(oxidized)}$ ratio in microcosms amended with only nitrate remained similar at a value of 5, indicating no mechanistic change in the reduction of nitrate. In contrast, in microcosms

amended with both nitrate and Fe(II), the reduction of 2 mM nitrate was coupled to the oxidation of less than 0.1 mM Fe(II) after the nitrate spike on day 60 ($NO_3^-{}_{[reduced]}$/$Fe[II]_{[oxidized]}$ ratio of 20). In microcosms amended with both nitrate and Fe(III) but lacking addition of Fe(II), nitrate reduction started heterotrophically on day 0. When nitrate was completely removed, Fe(III) reduction started and provided a supply of Fe(II) (Fig. 3E). Subsequently, after a second nitrate spike on day 60, the reduction of 2 mM nitrate was coupled to the oxidation of approximately 2.4 mM Fe(II), corresponding to an $NO_3^-{}_{(reduced)}$/$Fe(II)_{(oxidized)}$ ratio of 0.8.

Role of cryptic Fe cycling for Fe(II) oxidation in freshwater sediments amended with nitrate. One additional factor that could potentially influence the measurable ratio of $NO_3^-{}_{(reduced)}$/$Fe(II)_{(oxidized)}$ is cryptic Fe cycling (32, 33). Cryptic element cycling refers to rapid turnover of redox species that occurs too fast to be detected, but which ultimately alters the measured budgets of involved electron donors and terminal electron acceptors. In our setups, the immediate rereduction of Fe(III) produced by Fe(II) oxidation might lead to overestimation of the $NO_3^-{}_{(reduced)}$/$Fe(II)_{(oxidized)}$ ratio, i.e., the actual amount of Fe(II) oxidized could be higher than determined based on the present Fe(II) concentrations. The fact that Fe(III) reduction started instantaneously after complete nitrate reduction, which is required for Fe(II) oxidation, suggests cryptic Fe cycling in most biotic setups, i.e., Fe(III) is probably also reduced during the time period when we see a net Fe(II) oxidation. This allows a relative comparison of the ratios and, consequently, a determination of the impact of autotrophic nitrate-dependent Fe(II) oxidation. In microcosms amended with nitrate and Fe(III), reduction of Fe(III) started only after a lag phase of 6 days after nitrate reduction was finished, indicating the absence of cryptic Fe cycling during nitrate reduction in these setups.

Impact of DOC on Fe(II) oxidation in freshwater sediment. The high $NO_3^-{}_{(reduced)}$/$Fe(II)_{(oxidized)}$ ratio in microcosms amended with nitrate and Fe(II) coincides with a high present DOC concentration (17 mg per liter at day 45 compared to 11 mg per liter at day 0), indicating that at this point, nitrate reduction was performed almost exclusively heterotrophically. In microcosms amended with nitrate and Fe(III) that lacked the initial supply of Fe(II), nitrate reduction started, probably heterotrophically, on day 0. However, after a nitrate spike on day 60, the low $NO_3^-{}_{(reduced)}$/$Fe(II)_{(oxidized)}$ ratio of 0.8 indicates an increased utilization of Fe(II) as electron donor by autotrophic or mixotrophic nitrate-reducing Fe(II) oxidizers. Considering the very low DOC concentration of only 3 mg per liter at this time point, a strong impact of mixotrophic or even autotrophic nitrate-reducing Fe(II) oxidizers is indicated. This is also indicated by the rates of nitrate-reducing Fe(II) oxidation measured in different setups and at different DOC concentrations. The highest rate of nitrate-dependent Fe(II) oxidation, 154.8 $\pm$ 36.2 μM per day, coincided with a DOC concentration of 3.2 $\pm$ 0.6 mg per liter in microcosms amended with Fe(III) and nitrate after the nitrate spike on day 60. With increasing DOC concentration, the Fe(II) oxidation rate consistently dropped. At a DOC concentration of 10.7 $\pm$ 0.6 mg per liter in microcosms amended with Fe(II) and nitrate from the start of the experiment, the rate of nitrate-reducing Fe(II) oxidation was only 15.0 $\pm$ 6.7 μM per day. At the highest DOC concentration of 21.8 $\pm$ 2.5 mg per liter measured in microcosms amended with Fe(II) and nitrite, no Fe(II) oxidation was observed. This implies that heterotrophic nitrate reduction is favored by the nitrate-reducing bacterial community, yet under carbon-limited conditions Fe(II) can be used as electron donor. In addition, low DOC levels would limit Fe(III) reduction, which would also lead to a higher net Fe(II) oxidation rate. These findings coincide with the results of Laufer et al. (31), strengthening the interpretation that under low concentration of DOC the use of electrons from Fe(II) oxidation for the autotrophic reduction of nitrate becomes increasingly important. This is particularly important for environments with fluctuating DOC content, such as lake sediments, and for agriculturally used soils where high nitrate inputs and subsequent consumption might lead to a depletion of DOC.

Microbially mediated Fe(II) oxidation coupled to nitrate reduction in freshwater sediments. Because all Fe(II) oxidation rates measured in biotic setups have to be

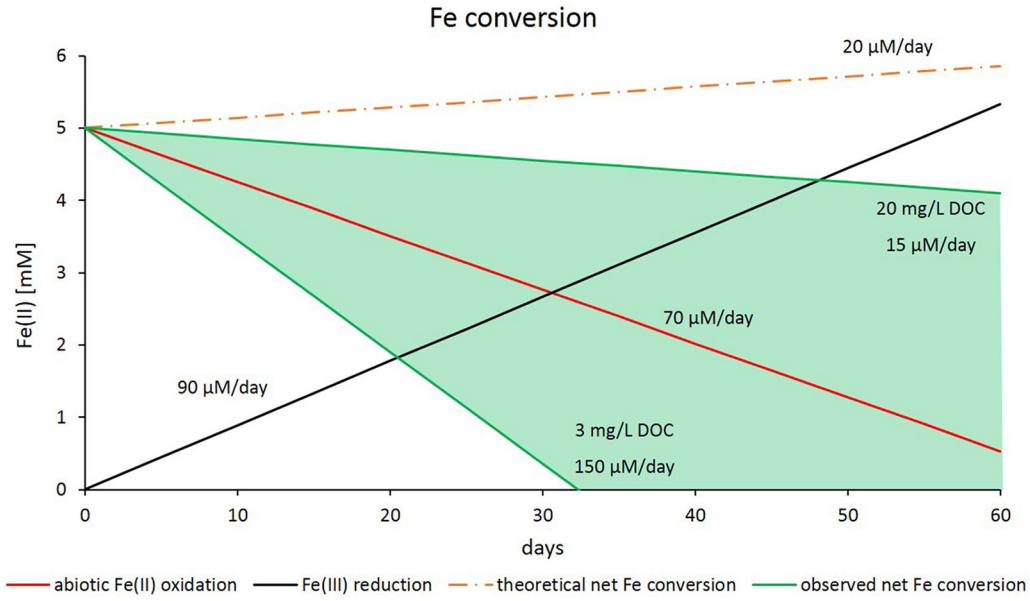

FIG 7 Fe conversion rates (i.e., net rates displaying simultaneous Fe[II] oxidation and Fe[III] reduction) dependent on DOC content, as determined from microcosm experiments amended with 5 mM Fe(II) or Fe(III) and 2 mM nitrate or nitrite. The theoretical net Fe conversion displays the assumption that Fe(II) oxidation would happen abiotically only by reaction with nitrite. The difference between the theoretical net Fe conversion (orange dotted line) and the actual measured Fe conversion (green marked range) represents the contribution of microbially catalyzed Fe(II) oxidation coupled to nitrate reduction.

considered net rates, which include the biotic and abiotic oxidation of Fe(II) as well as the reduction of Fe(III), we tried to assess the proportions of the individual processes. The rate of Fe(II) oxidation resulting from the abiotic reaction with nitrite could be determined in microcosms with sediment that was sterilized by autoclaving. Additionally, biotic Fe(III) reduction rates were considered to display only Fe(III) reduction because Fe(II) oxidation was expected to be impossible due to the lack of nitrate, nitrite, light, or oxygen. Summing up the rates of biotic Fe(III) reduction and abiotic Fe(II) oxidation by nitrite resulted in the theoretical net Fe conversion rate that is displayed in Fig. 7. All measured Fe conversion rates from different microcosm setups showed faster Fe(II) oxidation over time than that suggested by the calculated net Fe conversion rate. This implies that in addition to the abiotic side reaction with nitrite, Fe(II) oxidation is coupled to active nitrate reduction, even in setups with high DOC concentration where Fe(II) oxidation coupled to nitrate reduction plays a minor role compared to that in heterotrophic nitrate reduction. The negative correlation of the DOC concentration and the proportion of Fe(II) oxidation coupled to nitrate reduction indicates a high impact of microbially mediated processes for the coupling of nitrate reduction and Fe(II) oxidation.

Copy numbers of genes encoding nitrate and nitrite reductases revealed the same trends as for 16S rRNA genes, indicating that none of the substrate amendments caused significant changes in abundances of denitrifying bacteria. Gene expression levels, however, clearly varied between different setups and over time. First of all, expression levels of all nitrate and nitrite reductases stayed stable after nitrate amendment, whereas they dropped without this amendment. This indicates that the natural lake sediment is constantly supplied with nitrate, which is immediately consumed by bacteria and thus is barely measurable in the sediment or the overlying water column. Setups amended with Fe(II) showed elevated expression levels of nitrate- and nitrite-reductase-encoding genes (Fig. 6A). This correlates with results of former studies, which reported enhanced nitrate reduction rates in the presence of Fe(II) (15, 17); in addition, we could link this increased nitrate reduction to enhanced gene expression, possibly caused by the presence of Fe(II). The effects of high Fe(III) concentrations on the

expression of nitrate- and nitrite-reductase-encoding genes could not be determined. The decreased Fe(II) oxidation rates in the setups amended with Fe(III) could be caused by either downregulation of nitrate and nitrite reductases or by competition for organic carbon between nitrate- and Fe(III)-reducing bacteria. However, it could also be explained by an inhibitory effect due to Fe(III) reduction (34). The strongest effect on the expression of nitrate- and nitrite-reductase encoding genes was found in setups amended with Fe(II) and nitrite. This is especially remarkable, as by the time samples for DNA/RNA quantification were taken, nitrite had already been removed from the aqueous phase for several days. Still, RNA for the nitrite reductase was expressed. As mRNA has only a short half-life (35, 36), the continuous expression of the nitrite reductase (even in the absence of nitrite) might be due to an ongoing stress response towards nitrate toxicity (37, 38).

Implications for the existence of microbially mediated nitrate-reducing Fe(II) oxidation. With the discovery of Fe(II) oxidation coupled to nitrate reduction (8), the question arose of whether or not this metabolism is mainly driven by biotic or abiotic processes. The dependence of Fe(II) oxidation on nitrate reduction shown in many studies led to the conclusion that both processes are enzymatically coupled. Nevertheless, many isolated nitrate-dependent Fe(II) oxidizers need an organic cosubstrate for growth. In combination with the observation that ordinary nitrate-reducing bacteria can potentially oxidize Fe(II) (17, 19, 21, 39) abiotically by reactive nitrogen species produced during denitrification, these observations cast doubt on whether an enzymatic coupling of nitrate reduction and Fe(II) oxidation truly exists. Additionally, recent studies demonstrate the existence of autotrophic nitrate-reducing Fe(II) oxidizers in marine sediments (30), and our findings reveal an influence of Fe(II) on the expression of genes encoding enzymes responsible for denitrification. From these findings we conclude that Fe(II) oxidation coupled to nitrate reduction is mainly a microbially mediated process. Future studies could focus on DNA-SIP (stable isotope probing) to determine the community members utilizing this type of metabolism or on nano-SIMS (nanoscale secondary-ion mass spectrometry) experiments in enriched or pure cultures to unravel the underlying mechanism of nitrate-reducing Fe(II) oxidation.

MATERIALS AND METHODS

Sampling site and sampling procedure. Littoral sediment and water samples were taken in September 2015 and February 2016 at Lake Constance, a freshwater lake in southern Germany, at a location in the northwestern arm known as the Überlingersee, which is near the island of Mainau at 47°41′42.63′′N and 9°11′40.29′′E, at a water depth of 0.5 to 1.0 m. Temperature, pH, salinity, and oxygen saturation of the water were measured directly at the site with a field multimeter (Multi 3430; WTW;) equipped with a pH electrode with a temperature sensor (SenTrix; WTW), a conductivity electrode (TetraCon92; WTW), and an oxygen sensor (FDO925; WTW). Sediment and water samples were transported to the laboratory at 4°C and the sediment was processed immediately for geochemical measurements and microcosm incubations.

Microelectrode measurements. In September 2015, microelectrode measurements were performed directly at the site, immediately after sediment sampling in 50-ml syringes (10 cm × 2.5 cm) with cutoff tips. High-resolution profiles of dissolved O_2, pH, and redox potential were measured with commercially available glass microelectrodes with a 100-μm tip diameter (Unisense, Denmark). Vertical profiles of oxygen were measured at a depth resolution of 200 μm, and all other parameters were determined at a resolution of 500 μm using a manual micromanipulator. Data were recorded with the software Sensor Trace Pro (Unisense, Denmark). Before and during measurements, the overlying water in the sediment cores was aerated, as the littoral surface sediment *in situ* is saturated with oxygen. For each parameter, triplicate profiles were measured in the same sediment core at different positions. Profiles of dissolved Fe^{2+} were obtained using a DLK-100A potentiostat (Analytical Instrument Systems, Flemington, NJ) with a standard three-electrode system. The working electrode was a 100-μm gold amalgam (Au/Hg) glass electrode which was constructed as described by Brendel and Luther (40). The reference electrode was an Ag wire coated in Ag/AgCl; a Pt wire was used as counter electrode. Working and reference electrodes were replated before the measurements. Fe^{2+} calibrations were done using Mn^{2+} standards with subsequent conversions to Fe^{2+} concentrations using the pilot ion method (40, 41). A pilot ion factor of 1.3 was determined. Cyclic voltammograms for Mn^{2+} and Fe^{2+} were collected by scanning from −0.1 V to −2.0 V and back to −0.1 V (versus Ag/AgCl) at a scan rate of 1,000 mV/s. An initial conditioning step of applying −0.05 V for 5 s, followed by holding at −0.9 V for 10 s, was set to remove previously deposited species (40). After the conditioning step, the electrode equilibrated for 5 s before scan potentials were applied. Ten scans were done at each measurement point, and the resulting voltammograms were integrated using the VOLTINT program for Matlab (42).

Sediment characterization. Water content of the littoral sediment was determined on a wet-weight basis in triplicate by weighing portions of wet sediment, drying them for 4 days at 80°C, and subsequently determining the dry weight. The elemental composition of the sediment was determined by X-ray fluorescence (XRF) analysis with a Bruker AXS S4 Pioneer X-ray fluorescence spectrometer and micro-X-ray diffraction (μXRD) (Bruker D8 Discover X-ray diffraction instrument; Bruker AXS GmbH, Germany). The samples were analyzed for DOC with a high-TOC Elementar instrument.

Microcosm setup. Lake water for the microcosm experiments was purged with N_2 gas for 1 h, sterile-filtered (0.22 μm, mixed ester cellulose membrane) under an N_2 atmosphere in a glove box, and buffered with 22 mM bicarbonate buffer. The pH of the water was adjusted with sterile anoxic 1 M HCl to pH 7.6, which was the pH measured in the original lake water before purging. Hundred-ml serum bottles were filled with 5 g of wet sediment and 50 ml of filter-sterilized lake water (to most closely mimic *in situ* conditions), sealed with a butyl rubber stopper, and crimped. The headspace was replaced by N_2/CO_2 (90:10, vol/vol) gas. To inhibit microbial sulfate reduction, sterile anoxic Na_2MoO_4 solution was added to a final concentration of 1 mM. Additional additives (all sterile and anoxic) were added to the lake water in the following concentrations and in various combinations, i.e., 5 mM Fe(II) ($FeCl_2$), 2 mM NO_2^- ($NaNO_2$), 2 mM NO_3^- ($NaNO_3$), and 5 mM Fe(III) (ferrihydrite prepared according to Cornell and Schwertmann; 1). Two sets of abiotic controls were run. In one set, microbial activity was inhibited by addition of NaN_3 at a final concentration of 160 mM. Due to the removal of nitrite by NaN_3, a second control was prepared using sediment that was autoclaved anoxically for 3 times within 3 days. All setups were run in triplicate. Additional sacrificial triplicates of the biotic setups were prepared for DNA/RNA extraction at two time points during incubation. The microcosms were incubated at 26°C in the dark for 90 days.

Subsampling and analysis of microcosm incubations. One milliliter of sediment slurry was sampled from each microcosm at each sampling point using a sterile anoxic syringe and needle (inner diameter of 1.20 mm) in an anoxic glove box under N_2 atmosphere, without opening the bottles. Of the sampled slurry, 100 μl was stabilized in 900 μl of 40 mM sulfamic acid/1 M HCl (14, 43) and incubated in the dark on a shaker for 1 h at 150 rpm. The samples were then centrifuged for 5 min at 15.4 $\times$ *g* and the supernatant was used for the spectrophotometric ferrozine assay (44) in a spectrophotometric plate reader (MultiScan, Thermo Scientific, USA) to quantify Fe(II) and, after complete reduction of Fe(III) by hydroxylamine hydrochloride, Fe(total). The remaining slurry samples were centrifuged for 5 min at 15.4 g. The supernatant was diluted 1:10 in Milli-Q water and stored anoxically at 4°C for a maximum of 3 days before measurement of dissolved NO_3^-/NO_2^{--} by a flow injection analysis (FIA) system (3-QuAAtro; Bran+Lübbe, Norderstedt, Germany). At two time points during the microcosm incubation, after complete nitrate/nitrite removal in all setups and after Fe (re)reduction in all setups, sacrificial microcosms were harvested. Overlying water was frozen at −80°C in organic-free gas chromatography (GC) vials (burned for 5 h at 450°C) and closed with screw-caps with a polytetrafluoroethylene (PTFE) inlet for analysis of volatile fatty acids (VFA), and sediment of triplicate microcosms was pooled and homogenized. The sediment was fixed with LifeGuard soil preservation solution (dianova GmbH, Hamburg, Germany) and frozen at −80°C for total DNA/RNA extraction.

Analysis of VFAs by 2-dimensional ion chromatography-mass spectrometry. Prior to analysis, the water samples treated as described above were thawed and filtered through disposable syringe filters (Acrodisc ion chromatography [IC] grade, 0.2 mm pore size, 13 mm diameter). The syringe filters were cleaned by rinsing with 10 ml of Milli-Q water (Ultrapure, type I) directly before use. The first 0.5 ml of filtered sample was discarded and the next 0.5 ml was used for VFA analysis. All samples were analyzed directly without dilution. Samples with high acetate concentrations (above 100 μM) were additionally analyzed after 1:10 dilution with Milli-Q water. VFAs were analyzed by 2-dimensional ion chromatography-mass spectrometry (2D IC-MS), as described in detail in Glombitza et al. (45) and Laufer et al. (31) with some modifications with respect to the low salinity of the lake water samples. The instrument used was a dual Dionex ICS3000 ion chromatograph coupled to an MSQ Plus mass spectrometer (Thermo Scientific). The first IC dimension is used to separate the bulk VFAs from the inorganic ions of the sample matrix (i.e., the incubation medium). To account for the slightly different retention times of the VFAs in low salinity samples compared to in the saline samples for which the analysis protocol was initially developed, the retention time window directed to the trap column was shifted to 4 to 8.5 min. During this interval, the VFAs were trapped on a concentrator column (Dionex Ion-Pac UTAC-ULP1; Thermo Scientific) and subsequently separated in the second IC dimension. The column for the first dimension was a Dionex IonPac AS24, and for the second dimension a Dionex IonPac AS11HC (both from Thermo Scientific). Blank measurements of Milli-Q water (Ultrapure, type I) were used to correct for background. Quantification was done by comparing the peaks to the peaks from external standard mixtures of all analyzed VFAs at three different concentrations (200, 500, and 800 μg per liter). Detection limits for the individual VFAs were between 0.1 and 0.5 μM. For a detailed discussion of analytical and statistical parameters (detection limits, sensitivity, accuracy, and precision) see Glombitza et al. (45).

DNA/RNA extraction. Total DNA and RNA were extracted using the RNA PowerSoil Total RNA isolation kit and RNA PowerSoil DNA Elution accessory kit (Mo Bio Laboratories Inc., Carlsbad, CA, USA). DNA samples were stored at −20°C. RNA samples were further processed with the Turbo DNA-free kit (Invitrogen, Carlsbad, CA, USA) to remove DNA contaminations. For successful removal of DNA, the protocol for rigorous treatment was followed. The purified RNA was transcribed into cDNA using Superscript III Reverse Transcriptase (Invitrogen). cDNA samples were stored at −20°C.

Real-time quantitative PCR. To quantify relative abundances and activities of denitrifying microorganisms, Real-time quantitative PCR (qPCR) for the nitrate-reductase-encoding genes *napA* and *narG*

TABLE 1 Primers and protocols used for the quantification of functional genes encoding nitrate reductases (*napA* and *narG*), nitrite reductases (*nirK* and *nirS*), and bacterial 16S rRNA

Gene	Primer	Amplicon length (bp)	Reference	Reaction mixture	Thermal profile
napA	V17 m TGGACVATGGGYTTYAAYC napA4r ACYTCRCGHGCVGTRCCRCA	152	46	5 μl SsoAdvanced Universal SYBR, 0.5 μl V17 m (5 μM), 0.5 μl napA4r (5 μM), 3 μl PCR water, 1 μl template	15 s at 98°C, 15 s at 55°C, 15 s at 72°C × 45 cycles
narG	narG-f TCGCCSATYCCGGCSATGTC narG-r GAGTTGTACCAGTCRGCSGAYTCSG	173	46	5 μl SsoAdvanced Universal SYBR, 0.5 μl narG-f (5 μM), 0.5 μl narG-r (5 μM), 3 μl PCR water, 1 μl template	10 s at 98°C, 20 s at 62°C × 40 cycles
nirK	nirK876c ATYGGCGGVCAYGGCGA nirK1040 GCCTCGATCAGRTTRTGGTT (modified)	164	47	5 μl SsoAdvanced Universal SYBR, 0.5 μl nirK876c (5 μM), 0.5 μl nirK1040 (5 μM), 3 μl PCR water, 1 μl template	10 s at 98°C, 20 s at 58°C × 40 cycles
nirS	nirSCd3aF AACGYSAAGGARACSGG nirSRcd GASTTCGGRTGSGTCTTSAYGAA	407	48	5 μl SsoAdvanced Universal SYBR, 1 μl nirSCd3aF (5 μM), 1 μl nirSRcd (5 μM), 2 μl PCR water, 1 μl template	30 s at 98°C, 30 s at 57°C, 30 s at 72°C × 40 cycles
16S rRNA gene	341f CCTACGGGAGGCAGCAG 797r GGACTACCAGGGTATCTAATCCTGTT	456	49, 50	5 μl SsoAdvanced Universal SYBR, 1 μl 341f (5 μM), 1 μl 797r (5 μM), 2 μl PCR water, 1 μl template	5 s at 98°C, 12 s at 60°C, 1 min at 95°C × 40 cycles

as well as for the nitrite-reductase-encoding genes *nirK* and *nirS* were performed on DNA and cDNA samples. qPCR analyses were run on an iQ5 Real-Time PCR cycler (Bio-Rad Laboratories GmbH, Germany) using SsoAdvanced UniversalSYBRGreen Supermix (Bio-Rad). Primers and protocols used are listed in Table 1.

SUPPLEMENTAL MATERIAL

Supplemental material for this article may be found at https://doi.org/10.1128/AEM.02013-17.

SUPPLEMENTAL FILE 1, PDF file, 0.2 MB.

ACKNOWLEDGMENTS

This work was funded by a DFG grant to A.K. (KA 1736/26-1), an ERC grant to A.K. (agreement number 307320—MICROFOX), a Margarete von Wrangell grant to C.S., and a Marie-Curie Individual Fellowship to C.G. (IEF, EU FP7, agreement 327675-DEEP CARBON FLUX).

We specially thank Ellen Roehm from the University of Tübingen, Germany, and the limnology team from the University of Konstanz, Germany, and Bernhard Schink, Konstanz, for critically reading the manuscript.

REFERENCES

1. Cornell RM, Schwertmann U. 2003. The iron oxides, 2nd ed. Wiley-VCH, Weinheim, Germany.
2. Kappler A, Emerson D, Gralnick JA, Roden EE, Muehe EM. 2016. Geomicrobiology of iron, p 343–399. *In* Ehrlich HL, Newmann DK, Kappler A (ed), Ehrlich's geomicrobiology, 6th ed. Taylor and Francis Group, Boca Raton, FL.
3. Melton ED, Swanner ED, Behrens S, Schmidt C. 2014. The interplay of microbially mediated and abiotic reactions in the biogeochemical Fe cycle. Nat Rev Microbiol 12:797–809. https://doi.org/10.1038/nrmicro3347.
4. Roden EE. 2012. Microbial iron-redox cycling in subsurface environments. Biochem Soc Trans 40:1249–1256. https://doi.org/10.1042/BST20120202.
5. Lovley DR, Phillips EJP. 1986. Organic matter mineralization with reduction of ferric iron in anaerobic sediments. Appl Environ Microbiol 51:683–689.
6. Emerson D, Moyer C. 1997. Isolation and characterization of novel iron-oxidizing bacteria that grow at circumneutral pH. Appl Environ Microbiol 63:4784–4792.
7. Ehrenreich A, Widdel F. 1994. Anaerobic oxidation of ferrous iron by purple bacteria, a new type of phototrophic metabolism. Appl Environ Microbiol 60:4517–4526.
8. Straub KL, Benz M, Schink B, Widdel F. 1996. Anaerobic, nitrate-dependent microbial oxidation of ferrous iron. Appl Environ Microbiol 62:1458–1460.
9. Blöthe M, Roden EE. 2009. Microbial iron redox cycling in a circumneutral-pH groundwater seep. Appl Environ Microbiol 75:468–473. https://doi.org/10.1128/AEM.01817-08.
10. Lovley DR. 1991. Dissimilatory Fe(III) and Mn(IV) reduction. Microbiol Rev 55:259–287.
11. Borch T, Kretzschmar R, Kappler A, Van Cappellen P, Ginder-Vogel M, Voegelin A, Campbell K. 2010. Biogeochemical redox processes and their impact on contaminant dynamics. Environ Sci Technol 44:15–23. https://doi.org/10.1021/es9026248.
12. Vaughan DJ, Lloyd JR. 2011. Mineral-organic-microbe interactions: Environmental impacts from molecular to macroscopic scales. Comptes Rendus Geosci 343:140–159. https://doi.org/10.1016/j.crte.2010.10.005.
13. Chakraborty A, Roden EE, Schieber J, Picardal FW. 2011. Enhanced growth of *Acidovorax* sp. strain 2AN during nitrate-dependent Fe(II) oxidation in batch and continuous-flow systems. Appl Environ Microbiol 77:8548–8556. https://doi.org/10.1128/AEM.06214-11.
14. Klueglein N, Kappler A. 2013. Abiotic oxidation of Fe(II) by reactive nitrogen species in cultures of the nitrate-reducing Fe(II) oxidizer *Acidovorax* sp. BoFeN1 - questioning the existence of enzymatic Fe(II) oxidation. Geobiology 11:180–190. https://doi.org/10.1111/gbi.12019.
15. Chakraborty A, Picardal FW. 2013. Induction of nitrate-dependent Fe(II) oxidation by Fe(II) in *Dechloromonas* sp. strain UWNR4 and *Acidovorax* sp. strain 2AN. Appl Environ Microbiol 79:748–752. https://doi.org/10.1128/AEM.02709-12.
16. Coby AJ, Picardal FW, Shelobolina E, Xu H, Roden EE. 2011. Repeated anaerobic microbial redox cycling of iron. Appl Environ Microbiol 77:6036–6042. https://doi.org/10.1128/AEM.00276-11.
17. Muehe EM, Gerhardt S, Schink B, Kappler A. 2009. Ecophysiology and the energetic benefit of mixotrophic Fe(II) oxidation by various strains of nitrate-reducing bacteria. FEMS Microbiol Ecol 70:335–343. https://doi.org/10.1111/j.1574-6941.2009.00755.x.
18. Straub KL, Schönhuber WA, Buchholz-Cleven BEE, Schink B. 2004. Diversity of ferrous iron-oxidizing, nitrate-reducing bacteria and their involvement in oxygen-independent iron cycling. Geomicrobiol J 21:371–378. https://doi.org/10.1080/01490450490485854.
19. Carlson HK, Clark IC, Blazewicz SJ, Iavarone AT, Coates JD. 2013. Fe(II) oxidation is an innate capability of nitrate-reducing bacteria that involves abiotic and biotic reactions. J Bacteriol 195:3260–3268. https://doi.org/10.1128/JB.00058-13.
20. Schädler S, Burkhardt C, Hegler F, Straub KL, Miot J, Benzerara K, Kappler A. 2009. Formation of cell-iron-mineral aggregates by phototrophic and nitrate-reducing anaerobic Fe(II)-oxidizing bacteria. Geomicrobiol J 26:93–103. https://doi.org/10.1080/01490450802660573.
21. Klueglein N, Zeitvogel F, Stierhof Y-D, Floetenmeyer M, Konhauser KO, Kappler A, Obst M. 2014. Potential role of nitrite for abiotic Fe(II) oxidation and cell encrustation during nitrate reduction by denitrifying bacteria. Appl Environ Microbiol 80:1051–1061. https://doi.org/10.1128/AEM.03277-13.
22. Nordhoff M, Tominski C, Halama M, Byrne JM, Obst M, Kleindienst S, Behrens S, Kappler A. 2017. Insights into nitrate-reducing Fe(II) oxidation mechanisms through analysis of cell-mineral associations, cell encrustation, and mineralogy in the chemolithoautotrophic enrichment culture KS. Appl Environ Microbiol 83:e00752-17. https://doi.org/10.1128/AEM.00752-17.
23. Weber KA, Pollock J, Cole KA, O'Connor SM, Achenbach LA, Coates JD. 2006. Anaerobic nitrate-dependent iron(II) bio-oxidation by a novel lithoautotrophic betaproteobacterium, strain 2002. Appl Environ Microbiol 72:686–694. https://doi.org/10.1128/AEM.72.1.686-694.2006.
24. Li B, Tian C, Zhang D, Pan X. 2014. Anaerobic nitrate-dependent iron (II) oxidation by a novel autotrophic bacterium, *Citrobacter freundii* strain PXL1. Geomicrobiol J 31:138–144. https://doi.org/10.1080/01490451.2013.816393.
25. Kumaraswamy R, Sjollema K, Kuenen G, van Loosdrecht M, Muyzer G. 2006. Nitrate-dependent [Fe(II)EDTA]$^{2-}$ oxidation by *Paracoccus ferrooxidans* sp. nov., isolated from a denitrifying bioreactor. Syst Appl Microbiol 29:276–286. https://doi.org/10.1016/j.syapm.2005.08.001.
26. Hafenbradl D, Keller M, Dirmeier R, Rachel R, Rossnagel P, Burggraf S, Huber H, Stetter KO. 1996. *Ferroglobus placidus* gen. nov., sp. nov., a novel hyperthermophilic archaeum that oxidizes Fe^{2+} at neutral pH under anoxic conditions. Arch Microbiol 166:308–314. https://doi.org/10.1007/s002030050388.

27. Su JF, Shao SC, Huang TL, Ma F, Yang SF, Zhou ZM, Zheng SC. 2015. Anaerobic nitrate-dependent iron(II) oxidation by a novel autotrophic bacterium, *Pseudomonas* sp. SZF15. J Environ Chem Eng 3:2187–2193. https://doi.org/10.1016/j.jece.2015.07.030.
28. Kiskira K, Papirio S, van Hullebusch ED, Esposito G. 2017. Fe(II)-mediated autotrophic denitrification: a new bioprocess for iron bioprecipitation/biorecovery and simultaneous treatment of nitrate-containing wastewaters. Int Biodeterior Biodegrad 119:631–648. https://doi.org/10.1016/j.ibiod.2016.09.020.
29. Mattes A, Gould D, Taupp M, Glasauer S. 2013. A novel autotrophic bacterium isolated from an engineered wetland system links nitrate-coupled iron oxidation to the removal of As, Zn and S. Water Air Soil Pollut 224.
30. Laufer K, Røy H, Jørgensen BB, Kappler A. 2016. Evidence for the existence of autotrophic nitrate-reducing Fe(II)-oxidizing bacteria in marine coastal sediment. Appl Environ Microbiol 82:6120–6131. https://doi.org/10.1128/AEM.01570-16.
31. Laufer K, Byrne JM, Glombitza C, Schmidt C, Jørgensen BB, Kappler A. 2016. Anaerobic microbial Fe(II) oxidation and Fe(III) reduction in coastal marine sediments controlled by organic carbon content. Environ Microbiol 18:3159–3174. https://doi.org/10.1111/1462-2920.13387.
32. Kappler A, Bryce C. 2017. Cryptic biogeochemical cycles: unravelling hidden redox reactions. Environ Microbiol 19:842–846. https://doi.org/10.1111/1462-2920.13687.
33. Berg JS, Michellod D, Pjevac P, Martinez-Perez C, Buckner CRT, Hach PF, Schubert CJ, Milucka J, Kuypers MMM. 2016. Intensive cryptic microbial iron cycling in the low iron water column of the meromictic Lake Cadagno. Environ Microbiol 18:1–41. https://doi.org/10.1111/1462-2920.13587.
34. Coby AJ, Picardal FW. 2005. Inhibition of NO_3^- and NO_2^- reduction by microbial Fe(III) reduction: evidence of a reaction between NO_2^- and cell surface-bound Fe^{2+}. Appl Environ Microbiol 71:5267–5274. https://doi.org/10.1128/AEM.71.9.5267-5274.2005.
35. Philippot L, Hallin S. 2005. Finding the missing link between diversity and activity using denitrifying bacteria as a model functional community. Curr Opin Microbiol 8:234–239. https://doi.org/10.1016/j.mib.2005.04.003.
36. Kushner SR. 2004. mRNA decay in prokaryotes and eukaryotes: different approaches to a similar problem. IUBMB Life 56:585–594. https://doi.org/10.1080/15216540400022441.
37. Bollag JM, Henninger NM. 1978. Effects of nitrite toxicity on soil bacteria under aerobic and anaerobic conditions. Soil Biol Biochem 10:377–381. https://doi.org/10.1016/0038-0717(78)90061-5.
38. Rajeev L, Chen A, Kazakov AE, Luning EG, Zane GM, Novichkov PS, Wall JD, Mukhopadhyay A. 2015. Regulation of nitrite stress response in *Desulfovibrio vulgaris* Hildenborough, a model sulfate-reducing bacterium. J Bacteriol 197:3400–3408. https://doi.org/10.1128/JB.00319-15.
39. Benz M, Brune A, Schink B. 1998. Anaerobic and aerobic oxidation of ferrous iron at neutral pH by chemoheterotrophic nitrate-reducing bacteria. Arch Microbiol 169:159–165. https://doi.org/10.1007/s002030050555.
40. Brendel PJ, Luther GW. 1995. Development of a gold amalgam voltammetric microelectrode for the determination of dissolved Fe, Mn, O_2, and S(-II) in porewaters of marine and freshwater sediments. Environ Sci Technol 29:751–761. https://doi.org/10.1021/es00003a024.
41. Slowey AJ, Marvin-DiPasquale MM. 2012. How to overcome interelectrode variability and instability to quantify dissolved oxygen, Fe(II), Mn(II), and S(-II) in undisturbed soils and sediments using voltammetry. Geochem Trans 13:1–20. https://doi.org/10.1186/1467-4866-13-6.
42. Bristow G, Taillefert M. 2008. VOLTINT: A Matlab-based program for semi-automated processing of geochemical data acquired by voltammetry. Comput Geosci 34:153–162. https://doi.org/10.1016/j.cageo.2007.01.005.
43. Schaedler F, Kappler A, Schmidt C. 2017. A revised iron extraction protocol for environmental samples rich in nitrite and carbonate. Geomicrobiol J 451:0–0.
44. Stookey LL. 1970. Ferrozine—a new spectrophotometric reagent for iron. Anal Chem 42:779–781. https://doi.org/10.1021/ac60289a016.
45. Glombitza C, Pedersen J, Røy H, Jørgensen BB. 2014. Direct analysis of volatile fatty acids in marine sediment porewater by two-dimensional ion chromatography-mass spectrometry. Limnol Ocean Methods 12:455–468. https://doi.org/10.4319/lom.2014.12.455.
46. Bru D, Sarr A, Philippot L. 2007. Relative abundances of proteobacterial membrane-bound and periplasmic nitrate reductases in selected environments. Appl Environ Microbiol 73:5971–5974. https://doi.org/10.1128/AEM.00643-07.
47. Henry S, Baudoin E, López-Gutiérrez JC, Martin-Laurent F, Brauman A, Philippot L. 2004. Quantification of denitrifying bacteria in soils by *nirK* gene targeted real-time PCR. J Microbiol Methods 59:327–335. https://doi.org/10.1016/j.mimet.2004.07.002.
48. Kandeler E, Deiglmayr K, Tscherko D, Bru D, Philippot L. 2006. Abundance of *narG*, *nirS*, *nirK*, and *nosZ* genes of denitrifying bacteria during primary successions of a glacier foreland. Appl Environ Microbiol 72:5957–5962. https://doi.org/10.1128/AEM.00439-06.
49. Muyzer G, de Waal EC, Uitterlinden AG. 1993. Profiling of complex microbial populations by denaturing gradient gel electrophoresis analysis of polymerase chain reaction-amplified genes coding for 16S rRNA. Appl Environ Microbiol 59:695–700.
50. Nadkarni MA, Martin FE, Jacques NA, Hunter N. 2002. Determination of bacterial load by real-time PCR using a broad range (universal) probe and primer set. Microbiology 148:257–266. https://doi.org/10.1099/00221287-148-1-257.